PERGAMON

International Journal of Multiphase Flow 26 (2000) 1493–1507

International Journal of Multiphase Flow

www.elsevier.com/locate/ijmulflow

Measuring interfacial waves on film flowing down tube inner wall using laser focus displacement meter

Tomoji Takamasa [a,*], Kenji Kobayashi [b]

[a] *Department of Marine Engineering, Tokyo University of Mercantile Marine, Etchujima, Koto-ku, Tokyo, 135-8533, Japan*

[b] *Graduate School of Marine Engineering, Tokyo University of Mercantile Marine, Etchujima, Koto-ku, Tokyo, 135-8533, Japan*

Received 23 December 1998; received in revised form 3 September 1999

Abstract

To elucidate details of the fascinating nonlinear phenomena of waves on a film, spatial temporal knowledge of the interfacial waves is essential. This paper presents a new method for measuring waves on a film flowing down the inner wall of a vertical tube, using a laser focus displacement meter. The purpose of the study was to clarify the effectiveness of the new method for obtaining detailed information of film thickness or wave characteristics, and to investigate the effect of film entry length on the phenomena. With this method, accurate measurements of film thickness in real time, with sensitivity of 0.2 μm and 1 kHz, were achieved. The error caused by refraction of the laser beam passing through an acrylic tube, whose outer wall surface was flat, and water was estimated. As the entry length increased, the ripple on the flowing film grew to a solitary wave of about 0.5 mm in height, then the wave became a two-wave system. In the entry region, the wave amplitude decreased as the flow rate increased, in the same manner as that in a film flowing down a plate wall.

Keywords: Flow measurement; Local measurement; Laser-aided diagnostics; Free surface flow; Film; Interfacial wave; Pipe flow; Multiphase flow

* Corresponding author. Tel.: +81-3-5245-7406; fax: +81-3-5245-7336.
E-mail addresses: takamasa@ipc.tosho-u.ac.jp (T. Takamasa), 712xzl@ipc.tosho-u.ac.jp (K. Kobayashi).

0301-9322/00/$ - see front matter
PII: S0301-9322(99)00099-3

1. Introduction

In view of the great importance to elucidate the fascinating nonlinear phenomena of waves on a film, extensive measurements have been performed intensively in the past 20 years using electrical resistance or electrical capacity methods, a laser displacement sensor, a supersonic echo method, and other methods (Hewitt and Hall-Taylor, 1970; Mori et al., 1998; Nasr-Esfahany and Kawaji, 1996; Poltalski and Clegg, 1972; Serizawa et al., 1995). When applied to microscopic measurement, however, these methods have three inherent shortcomings. (1) Instantaneous crest and roughness of the wave cannot be measured by these methods, although the spatial average film thickness can be determined. (2) The probe disturbs the flow. (3) If the curvature of the wave is large or if the wave is small, the wave cannot be measured accurately.

In our previous study, interfacial waves on a film flowing down a vertical plate wall in a developing region were measured using laser focus-displacement meters (LFDs, Keyence Co. Japan, Model LT 8100) which were developed to detect scratches on electrical devices (Takamasa et al., 1997, 1998). The results can be summarized as follows:

1. The effectiveness of a new method using LFDs for obtaining detailed information on a film was clarified, and the effect of the length of the developing region on the wave phenomena was investigated.
2. The error caused by the refraction of the laser beam passing through a transparent plate wall was clarified.
3. The measured average film thickness and wave velocity agreed with those calculated using Nusselt's law, indicating the flow to be laminar in the entry region even at a high flow rate.
4. The results of wave velocity and maximum film thickness agreed well with previous experimental and theoretical studies. An empirical equation for the relationship between the maximum film thickness and the experimental settings was presented.

This report presents an experimental study using an LFD for measuring waves on a film flowing down the inner wall of a vertical tube. The purpose of the study was to clarify the effectiveness of the new method for obtaining detailed information on waves on a film flowing down a tube inner wall, which are more encountered in industrial applications than those on a film flowing down a plate wall, and to investigate the effect of film entry length on the phenomena. Although efforts were made in the past to study the phenomena of falling film in a fully developed region, 1–2 m below the inlet section, very few detailed measurements have been made of the phenomena in the entry region, which is considered more important for industrial design than for the fully developed region.

2. Calibration for refraction

The displacement of the target from the LFD can be determined by detecting displacement of an objective lens that is moved frequently by a diapason or a tuning fork, when the laser beam passing through the objective lens is focused on the target. The diameter of the beam spot on the target is 2 μm, and the spatial resolution is 0.2 μm. The temporal resolution, which depends on the frequency of the tuning fork, was 1.4 kHz on the original LFD. To reduce

measurement error in the system, the output signal from the LFD uses the average of two measurements. Temporal resolution of the present LFD system thus is 0.7 kHz. As a result, the tiniest roughness of a wave can be detected.

It is possible to measure a liquid film flowing down the inner wall of a transparent tube using the LFD from outside the tube. It is, however, necessary to estimate the displacement error caused by refraction of the laser beam passing through both sides of the tube surface. The errors caused by the refraction of a beam passing through a transparent plate were clarified in the previous report (Takamasa et al., 1998). The curvature of the tube wall causes another problem: when the conical laser beam from the LFD reaches the target on the film surface, the beam scatters and is reflected from the target back into the LFD. The beam passing through the wall in the direction of the tube diameter and the beam in the direction of the tube axis do not focus on the same spot. The brightness of the beam reflected from the spot towards the LFD is lower than the detection level of the light-sensor of the LFD, due to the widening and scattering of the beam. It is thus difficult for the LFD to measure the thickness of a film flowing on a tube inner wall when the usual tubular geometry is used. We did a preliminary test to identify an appropriate measuring method that would solve the problem described above. The preliminary test showed that the brightness of the light reflected from the surface of the film on the tube's inner wall was strong enough to be detected by the light-sensor when the wall's outer surface was flat, as shown in Fig. 1.

The LFD can measure the liquid and the plate surfaces in one movement cycle of the objective lens, and the film thickness can be calculated from the displacement difference between the two signals. First, the displacement error caused by refraction and scattering was examined theoretically using the law of refraction (Fig. 2). In the figure, the origin of the X (tangential direction), Y (diametric direction or conical beam direction), and Z (tube axis direction) axes is on the intersection of the tube's inner surface with the axis of the conical laser beam. The position of the beam passing through the wall or window in the direction of the tube axis y_Z is expressed by the following equation, which is a function of the measured

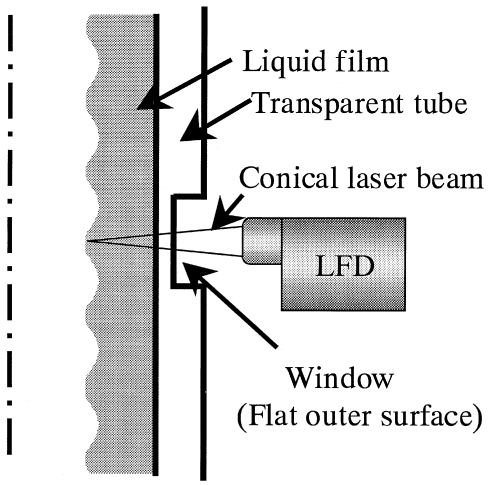

Fig. 1. Laser focus displacement meter.

film thickness δ_m, when water is used as the fluid. This equation is the same as that for a plate window (Takamasa et al., 1998).

$$y_Z = 1.33\delta_m \tag{1}$$

The position of the beam passing through the window in the tube diametric direction y_X is obtained as follows. The position of the light-path in the window is:

$$y = -\frac{1}{\tan\kappa_W}x + \frac{\tan\kappa_A}{\tan\kappa_W}\delta_m \tag{2}$$

where κ is the angle of incidence at the surface, and subscripts A and W represent air and window, respectively. The position on the inner surface of diameter D is:

$$y = \sqrt{\frac{D^2}{4} - x^2} - \frac{D}{2} \tag{3}$$

Refraction point $P(x_p, y_p)$ is obtained by the above equations. Tangential angle α is:

$$\alpha = \tan^{-1}\frac{x_p}{y_p} \tag{4}$$

From Snell's law:

$$N_W \sin\kappa_W = N_F \sin\kappa_F \tag{5}$$

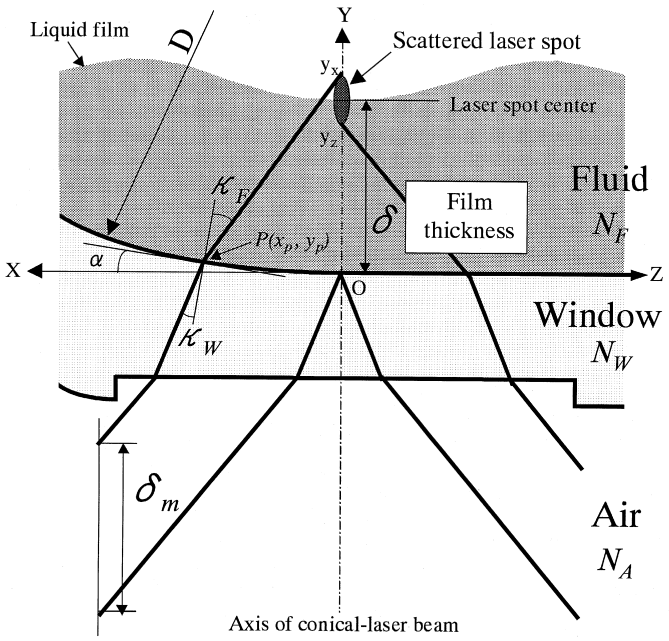

Fig. 2. Laser beam path.

where N is the refractive index and subscript F represents the fluid. The position of the conical-beam axis for the beam passing through the window in the diametric direction y_X is:

$$y_X = \frac{1}{\tan(\kappa_F + \alpha)} x_p + y_p \tag{6}$$

When the real target on the film surface is assumed to be in the center of the scattered beam, film thickness δ is:

$$\delta = \frac{(y_X + y_Z)}{2} \tag{7}$$

Substituting in the refractive indexes of acrylic window and water, $N_W = 1.49$ and $N_F = 1.32$, and the angle of incidence of a laser beam from the LFD to the target $\kappa_A = 11.5^\circ$, the real film thickness δ can be calculated from Eqs. (1)–(7).

$$\delta = \delta(N_W, N_F, \kappa_W, D, \delta_m) = \left(1.33 + 0.247\frac{\delta_m}{D}\right)\delta_m \tag{8}$$

This equation shows that the corrected film thickness δ is independent of the thickness of the window and the distance between the laser head and window when the film thickness is calculated from the displacement difference between the fluid and window surface.

Second, the displacement error was examined experimentally through a preliminary test. Fig. 3 illustrates the apparatus used in the preliminary test, which consisted of four pieces of acrylic tube, each cut in half horizontally and used as a flat-bottomed water tank. The inner diameters of the tubes, D, were 10, 15, 26, and 30 mm. The water depth which was equivalent

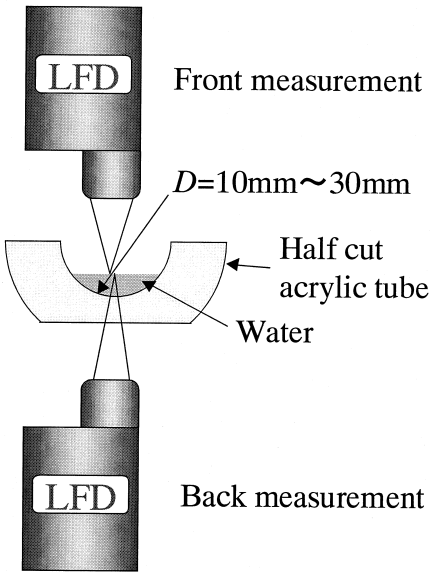

Fig. 3. Apparatus for the preliminary test.

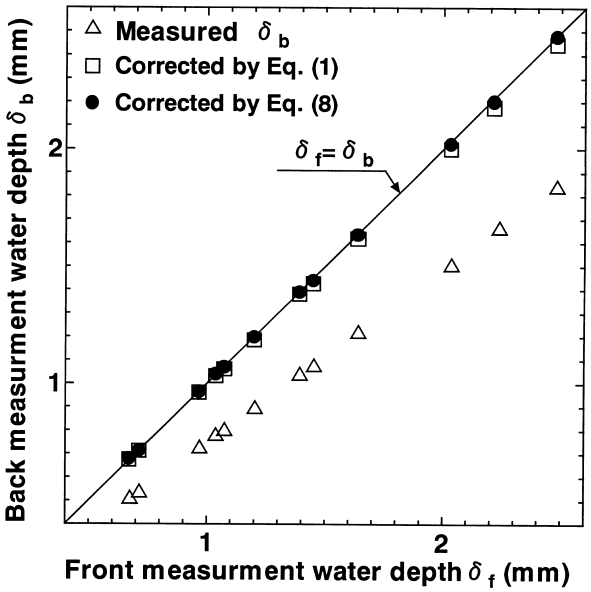

Fig. 4. Refraction error and corrected film thickness ($D = 26$ mm).

to the film thickness, was detected by LFDs positioned on the surface side (front measurement) and at the back of the wall (back measurement). Fig. 4 shows the relationship between the front measurement water depth δ_f and back measurement water depth δ_b. The open squares represent the corrected δ_b calculated by Eq. (1) which provides a correction without curvature. The corrected δ_b agrees with front measurement depth δ_f within a 5% margin of error, which is represented by a straight line in the figure. The solid circles represent the corrected δ_b calculated by Eq. (8) which provides a correction with curvature. The corrected δ_b agrees with δ_f within a 1.5% margin of error. To reduce the margin of error, theoretical equation (8) is modified using the experimental results which showed that real target was positioned slightly outside the center of laser spot. The following empirical equation was formulated by a curve fit to collapse the data using the least squares method.

$$\delta = \left(1.33 + 0.356\frac{\delta_m}{D}\right)\delta_m \tag{9}$$

The corrected δ calculated by Eq. (9) agrees with δ_f within a 1% margin of error as shown in Fig. 5. Eq. (9) is useful when $D = 10$–30 mm and $\delta = 0.5$–2.4 mm.

3. Apparatus

Fig. 6 shows the apparatus used in the present experiments. Water was purified to an electrical conductivity lower than 1.0 μS/cm by a pure water generator and pumped into a flowmeter, passing through a flow control valve and a head reservoir. After flowing down a

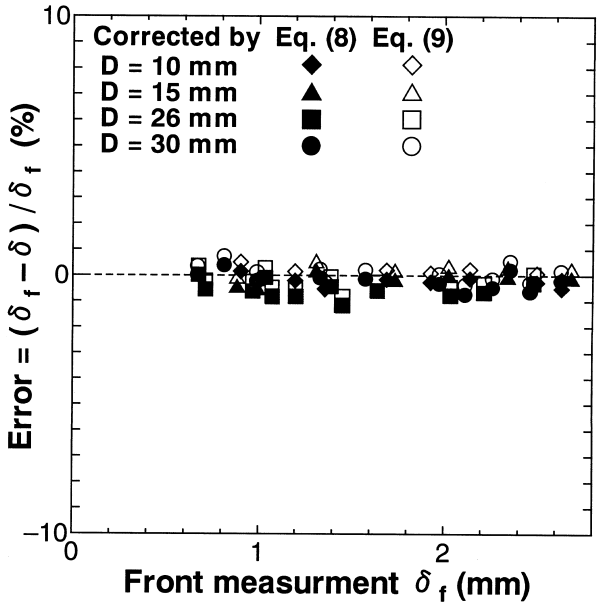

Fig. 5. Refraction error (D = 10–30 mm).

film generator through a test tube made of acrylic, the water flowed back to a water tank. A pressure accumulator was installed at the pump outlet to absorb oscillations caused by pump. A uniform liquid film was achieved by the use of a sintered metal tube as a film generator. The inside and outside diameters and length of the test tube were 26 mm, 32 mm and 3 m, respectively. The water temperature was maintained at a level of $25 \pm 0.3^{\circ}$C by a submerged heater and a cooler in the water tank. Two thermocouples in the water tank and in the film generator, were used to measure the water temperature. The experiments were performed with Reynolds number (Re) ranging from 80 to 3000, calculated from the volumetric flow rate Q, wetted perimeter πD and kinematic viscosity of the fluid $\nu(Re = \Gamma/\nu = Q/(\pi D\nu))$. The film thickness was measured using an LFD positioned at L = 216–2700 mm from the film entrance. The signal provided by the LFD was transmitted to a personal computer at a sampling frequency of 1 kHz. The phenomena was observed by a high-speed video camera operating at 2000 frames/s, synchronized with the wave measurement. A trigger signal started both the LFD and the camera.

In the experiments, long tube is used as the test section, tube oscillations caused by a pump or some driving device are inevitable. The oscillations may significantly affect the wave motion. The test section should therefore be rigid enough to reduce the oscillations, and oscillations should be checked to confirm the effect on the wave. In the present experiments, the LFD measured horizontal oscillations of the test section through all runs of the experiments and showed that the maximum amplitude of the oscillations had been smaller than 5 μm.

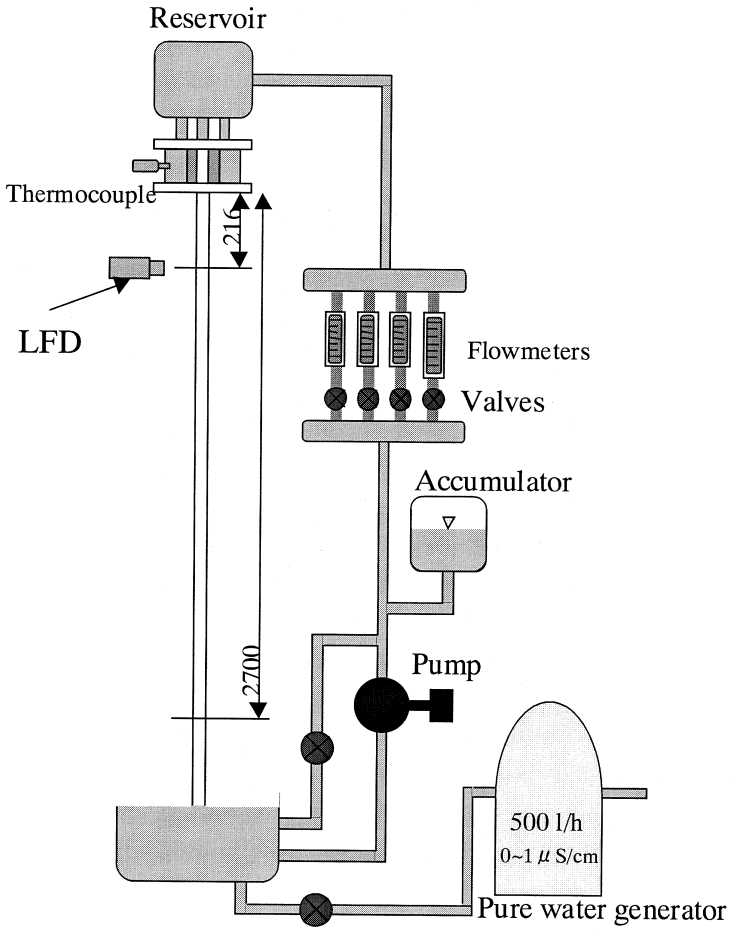

Fig. 6. Apparatus for the experiment.

4. Results

Fig. 7 shows the effects of entry length and liquid flow rate on the interfacial wave on a falling film. As shown in the figure, ripples smaller than 0.1 mm are formed on the interface at conditions of high Reynolds number and short entry length. The effect of flow rate on the probability density function of film thickness is shown in Fig. 8. Distribution of the function spreads over wide range of film thickness in the low flow rate condition with $Re = 80$, indicating a large wave amplitude of a solitary wave. The distributions are symmetrical and have almost identical sharp peaks with consistent width and height when $Re > 500$, indicating a wave amplitude that is small and independent of flow rate. As shown in Fig. 8, the ripple grows to a solitary wave about 0.5 mm in height with increasing of entry length. At entry length $L = 900$ mm, the wave becomes a two-wave system, as was also observed by Takahama and Kato (1980) in a fully developed region. In the entry region, $L = 216$ and 400 mm, the wave amplitude decreases as the flow rate increases, in the same manner as that in a film

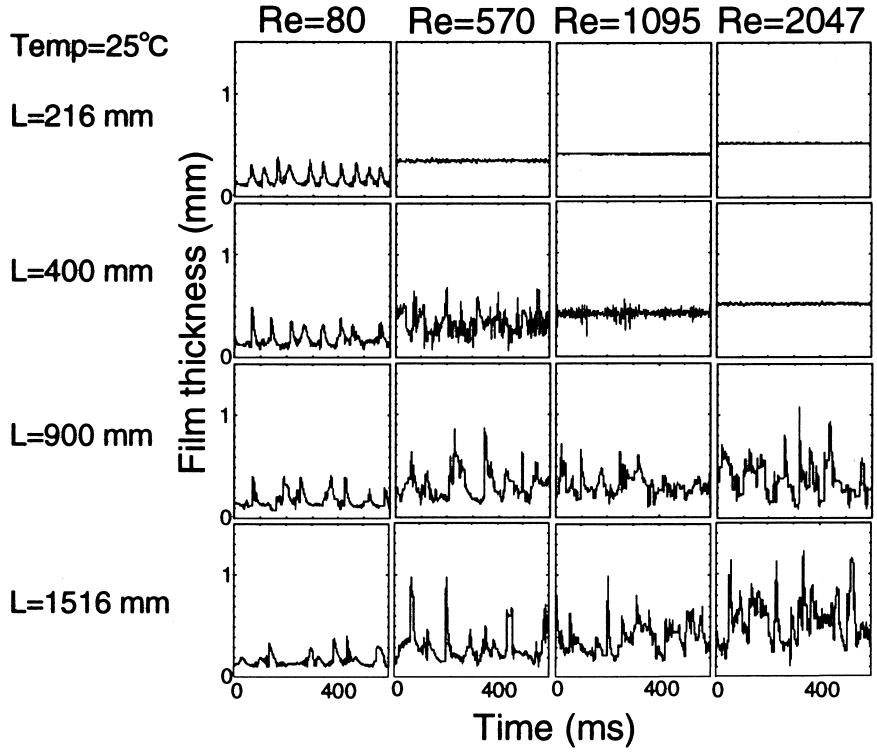

Fig. 7. Waves on a film flowing down a vertical tube inner wall.

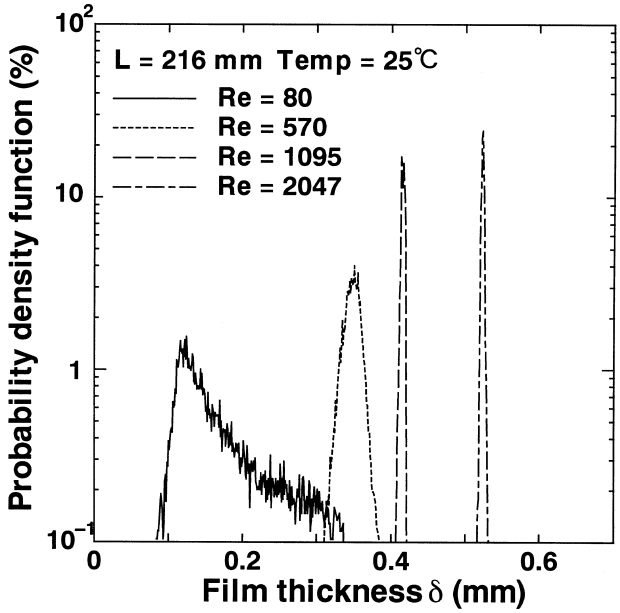

Fig. 8. Effect of flow rate on probability density function of film thickness.

flowing down a plate wall (Takamasa et al., 1998). The reason for this is that the time required to reach the measurement position becomes a key factor in the growth of the wave. As the flow rate or Reynolds number increases, the velocity of the flow increases, which shortens the time required to reach the measuring position. The wave, thus, cannot grow sufficiently if there is a high flow rate or a high Reynolds number. On the other hand, there is enough time for the waves to coalesce with each other and grow into a solitary wave under conditions of low flow rate.

The standard deviations of the film thickness affected by the entry length and flow rate are shown in Fig. 9. In low Reynolds number conditions, with $Re < 250$, the standard deviations, or wave roughness, is independent of entry length, and increase with Re. On the other hand, standard deviations are affected significantly by the entry length under high Reynolds number conditions, with $Re > 250$. The effect of entry length on the deviations becomes stronger as Re increases. At conditions of high Reynolds number, $Re > 1000$ and short entry length, $L < 400$ mm, the deviations are very small. High-speed video camera observation showed the film surface to be smooth as a mirror. Standard deviations increase and waves grow as the entry length increases. The growth does not stop, even at the long entry length conditions, $L = 2400$–2700 mm. This indicates that it is not suitable to assume the flow to be fully developed, for modeling flowing film in numerical analysis, when Re is greater than 250. The results of the standard deviations in a film flowing down a plate wall, measured using LFDs (Takamasa et al., 1998) and those flowing down a tube's inner wall measured by Mori et al. using electric probes (Mori et al., 1992) are plotted in the figure. The present results agree well with those in the plate wall experiments except in the case of very short entry condition, $L = 166.5$ mm. The discrepancy at the short entry condition could be caused by different film generators; the films

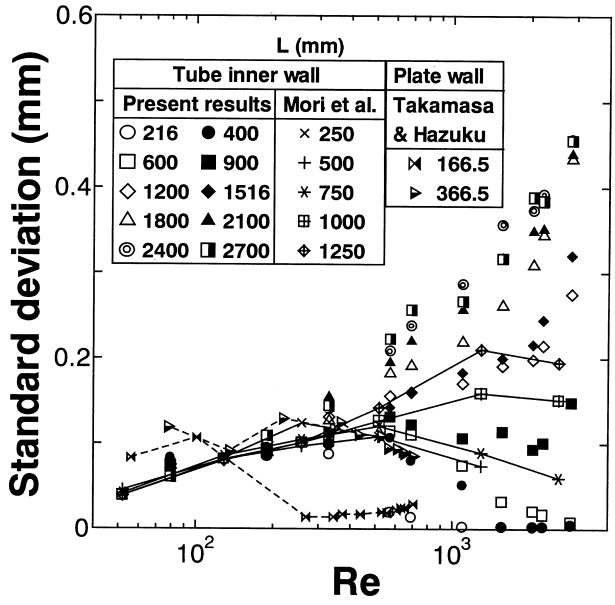

Fig. 9. Standard deviations in film thickness.

were generated by a slit in the plate wall experiment and by the sintered metal tube in the present experiments. The present results show fair agreement with Mori's results through all experimental settings.

Figs. 10–12 show the results of the calculations of the maximum film thickness δ_{max}, minimum film thickness δ_{min}, and average wave height $\bar{h}$. The minimum and maximum film thickness were calculated with a 1% and a 99% probability of film existence, respectively (Chu and Dukler, 1974). Arithmetically averaged distance h between the minimum film thickness and crest of each wave was defined as average wave height $\bar{h}$. Many empirical equations exist for calculating the minimum and maximum film thickness and average wave height of a film flowing down a vertical wall. In the figures, the solid lines are obtained by Ito–Sasaki's empirical equations for a film flowing down a vertical tube outer surface (Ito and Sasaki, 1986).

$$h_{max} = 1.78 \times 10^{-5} Re^{0.68} \tag{10}$$

$$\delta_{min} = 4.54\left(g/\nu^2\right)^{-1/3} \tag{11}$$

$$\delta_{max} = h_{max} + \delta_{min} \tag{12}$$

$$\bar{h} = 2.12 \times 10^{-5} Re^{0.53} \tag{13}$$

where g is the acceleration of gravity and ν is the kinematic viscosity of the fluid. Ito and

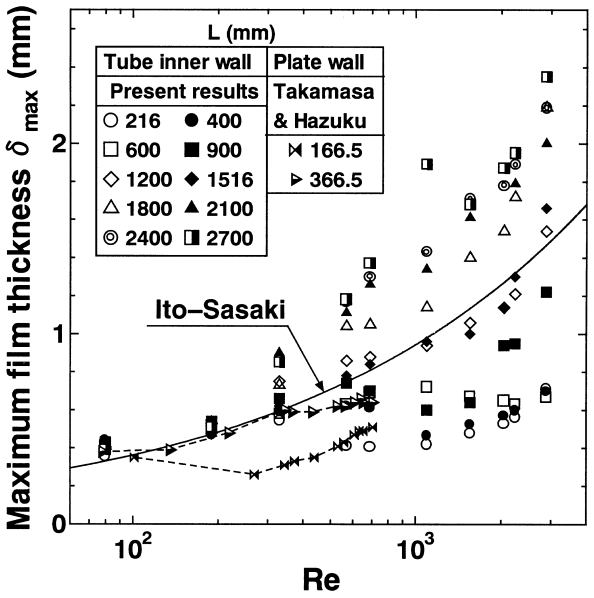

Fig. 10. Maximum film thickness.

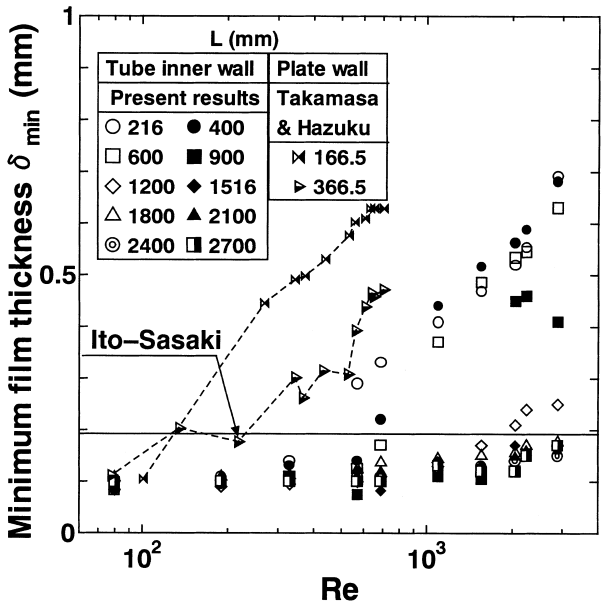

Fig. 11. Minimum film thickness.

Sasaki used a needle contact technique to measure the film thickness at 1600 mm from the film entrance.

As shown in Fig. 10, the present data for maximum film thickness δ_{max} are independent of entry length and increase with Re at low Reynolds number conditions, $Re < 250$. At high

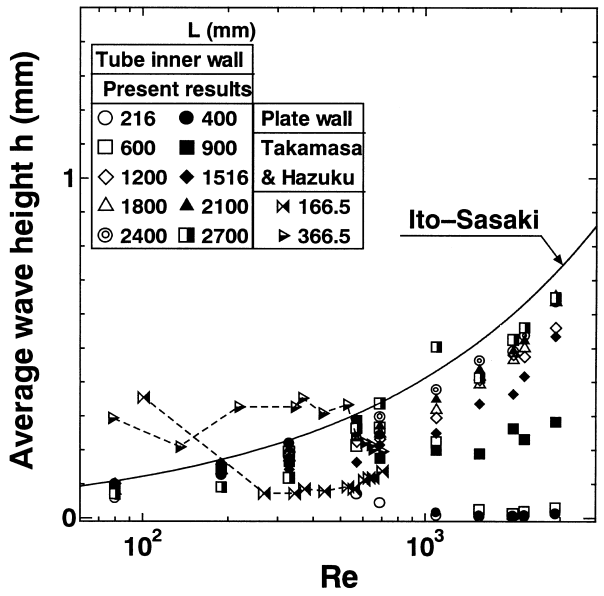

Fig. 12. Average wave height.

Reynolds numbers and short entry lengths, $Re < 900$ and $L = 216$–900 mm, the data have domains where the maximum film thickness decreases as Re increases. The reason for this has been explained qualitatively in the explanations for Figs. 7 and 8. As shown in the result for standard deviations, the waves grow as the entry length increases, and the growth does not stop even at long entry length conditions, with $L = 2400$–2700 mm. The present data agree fairly well with those calculated by Ito–Sasaki's equation at long entry conditions, with $L = 1516$ mm. This fact indicates that there is no difference between the needle contact measurements and the LFD measurements. Although the different film generators caused discrepancies between the present results and the plate wall experiments for $L = 166.5$ mm, the results of the maximum film thickness in the plate wall experiments agree with those in the present experiment when $L = 366.5$ mm. The fact that there are little difference among the results of the maximum film thickness in the plate wall, tube inner wall, and tube outer wall experiments indicates that we can ignore the effect of tube curvature on the behavior of falling film if the tube diameter is larger than 20–30 mm.

The minimum film thickness δ_{min} is independent of entry length in a manner similar to that of δ_{max} for low Reynolds numbers, with $Re < 250$ as shown in Fig. 11. At high Reynolds numbers, δ_{min} increases as the entry length decreases when $L < 1200$ mm, and it is independent of liquid flow rate or Re and entry length when $L > 1200$ mm. Takahama showed that the falling film became a fully developed turbulent flow when $L > 1300$ mm and $Re > 400$ (Takahama and Kato, 1980). His results show the same tendency as the present results for δ_{min} to be independent of flow rate and entry length at those settings. When $L > 400$ mm, δ_{min} in Takahama's results was around 0.2 mm, which agreed with those calculated by Ito–Sasaki's equation. This film thickness of 0.2 mm is greater than the present results, 0.1 mm. The reason for the discrepancy is that the needle contact technique may cause an error in minimum film thickness measurement by the needle's presence within the film, although it can measure the maximum film thickness accurately.

Fig. 12 shows that the effect of entry length on average wave height $\bar{h}$ is stronger as Re increases when $Re > 250$, in a manner similar to the results for standard deviations and δ_{max}. The wave grows from a mirror state in short entry conditions, with $L < 600$ mm to a very large wave in the long entry conditions, with $L = 2000$–2700 mm.

Fig. 13 shows the relationships between the average film thickness and Reynolds number as well as the entry length. The solid line in the figure represents a theoretical equation (14) in laminar flow conditions, calculated from Nusselt's Law (Nusselt, 1923).

$$\delta = \left(3\nu^2 Re/g\right)^{1/3} \tag{14}$$

The broken lines represent empirical equations obtained by Brauer (1956) (15), Takahama and Kato (1980) (16), and Aragaki et al. (1987) (17), respectively.

$$\bar{\delta} = 0.302\left(3\nu^2/g\right)^{1/3} Re^{0.526} \tag{15}$$

$$\bar{\delta} = 0.473\left(\nu^2/g\right)^{1/3} Re^{0.526} \tag{16}$$

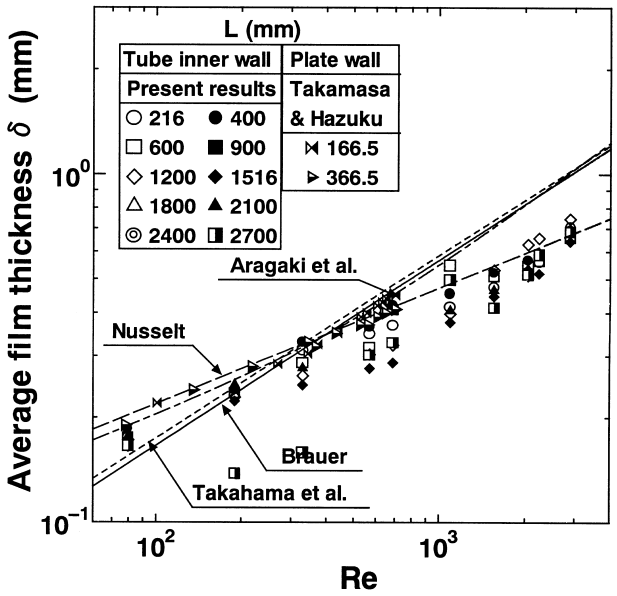

Fig. 13. Average film thickness.

$$\bar{\delta} = \left(\nu^2/g\right)^{1/3}\left[8.92Re^{5/2} + 4.04 \times 10^{-5}Re^{9/2}\right]^{2/15} \tag{17}$$

The present data agree well with Nusselt's theoretical equation in the short entry region. The boundary condition of the inlet in the present experiments differs from that in the theory. The former has a small horizontal velocity component of the liquid at the inlet of sintered metal, and the latter has not. The fact that the present data coincides with Nusselt's theory thus indicating that the flow is laminar even at a high flow rate and the horizontal velocity effects little on the flowing film. The results in the plate wall experiments that were carried out in a short entry region, with $L < 400$ mm, agree with those in the present experiments. The entry length affects the average film thickness when $Re > 250$ and the average film thickness tends to decrease as the entry length increases when $L < 1200$ mm, indicating the flow is underdeveloped. The effect of entry length is slight when $L > 1200$ mm.

5. Conclusion

This report presents an experimental study measuring waves on a film flowing down the inner wall of a vertical tube, using a laser focus displacement meter (LFD). The purpose of the study was to clarify the effectiveness of the new method for obtaining detailed information of waves on film flowing down a tube's inner wall and to investigate the effect on the phenomena of length from film entrance. The results are summarized as follows.

It was possible to measure the liquid film flowing down the inner wall of transparent tube using the LFD from the outside of the tube if the wall's outer surface was flat. The error caused by the refraction of the laser beam passing through the acrylic tube, whose outer wall

surface was flat, and water was estimated by Eq. (9). The results for minimum, maximum and average film thickness, as well as standard deviation of the film thickness, indicated that the wave behaviors was affected significantly by the entry length for high Reynolds numbers, with $Re > 250$. The waves grew as the entry length increased. The growth did not stop even at the long entry lengths, $L = 2400$–2700 mm. This fact indicated that it was not suitable, for modeling flowing film with Re greater than 250, to assume the flow to be fully developed. The fact that there was little difference among the results of maximum film thickness in the plate wall, tube inner wall, and tube outer wall experiments indicated that we could ignore the effect of the tube curvature on the falling film behavior if the tube diameter was larger than 20–30 mm.

Acknowledgements

The authors would like to thank Mr. T. Iguchi (Graduate School of Marine Engineering, Tokyo University of Mercantile Marine) for his help in conducting the experiments.

References

Aragaki, T., Toyama, S., Salah, H.M., Murase, K., Suzuki, M., 1987. Transitional zone in falling liquid film. Journal of Chemical Engineering Society (in Japanese) 13, 373–375.

Brauer, H., 1956. Strömung und Wärmeübergang bei Rieselfilmen, VDI-Forschungshelt 22–451.

Chu, K.J., Dukler, A.E., 1974. Statistical characteristics of thin, wavy films. AIChE Journal 20, 695–706.

Hewitt, G.F., Hall-Taylor, N.S., 1970. Annular Two-Phase Flow. Pergamon Press, Oxford.

Ito, A., Sasaki, M., 1986. Breakdown and formation of a liquid film flowing down an inclined plane. Transaction of the Japan Society of Mechanical Engineers (in Japanese) 52–475 B, 1261–1265.

Mori, K., Matsumoto, T., and Uematsu, H., 1998. Time-spatial interfacial structures and flow characteristics in falling liquid film. Proceedings of 3rd International Conference on Multiphase Flow, CD-Rom, #514.

Mori, K., Sekoguchi, K., Yoshida, A., Tsujino, H., 1992. Chaotic characteristics in time-varying thickness of falling liquid film. Transaction of the Japan Society of Mechanical Engineers (in Japanese) 58–550 B, 1838–1845.

Nasr-Esfahany, M., Kawaji, M., 1996. Turbulence structure under a typical shear induced wave at a liquid/gas interface. Proceedings of AIChE Symposium Series 310–92, 203–210.

Nusselt, W., 1923. Der Wärmeaustausch am Berieselungskühler. VDI-Z 67–9, 206–216.

Poltalski, S., Clegg, A.J., 1972. An experimental study of wave inception on falling liquid film. Chemical Engineering Science 27, 1257–1265.

Serizawa, A., Kamei, T., Kataoka, I., Kawara, Z., Ebisu, T., Torikoshi, K., 1995. Measurement of dynamic behavior of a liquid film flow with liquid droplets in a horizontal channel. Proceedings of 2nd International Conference on Multiphase Flow 2, 27–34.

Takahama, H., Kato, S., 1980. Longitudinal flow characteristics of vertical falling liquid film without concurrent gas flow. International Journal of Multiphase Flow 6, 203–215.

Takamasa, T., Hazuku, T., Kobayashi, K., 1997. Measurements of the interfacial waves on a film flowing down a vertical wall using laser focus displacement meters. Proceedings of Fifth Triennial International Symposium on Fluid Control, Measurement and Visualization 1, 189–194.

Takamasa, T., Tamura, S., and Kobayashi, K., 1998. Interfacial waves on a film flowing down plate wall in an entry region measured with laser focus displacement meters. Proceedings of 3rd International Conference on Multiphase Flow, CD-Rom, #453.